AD_____

Award Number:  W81XWH-12-1-0457

TITLE:  Noninvasive Detection and Differentiation of Axonal Injury/Loss, Demyelination, and Inflammation

PRINCIPAL INVESTIGATOR:   Sheng-Kwei Song

CONTRACTING ORGANIZATION:      Washington University
                                St. Louis, MO 63110-1010

REPORT DATE:  Uctoàer 2013

TYPE OF REPORT:  Annual

PREPARED FOR:  U.S. Army Medical Research and Materiel Command
                Fort Detrick, Maryland  21702-5012

DISTRIBUTION STATEMENT: Approved for Public Release;
                         Distribution Unlimited

The views, opinions and/or findings contained in this report are those of the author(s) and should not be construed as an official Department of the Army position, policy or decision unless so designated by other documentation.

# REPORT DOCUMENTATION PAGE

| 1. REPORT DATE | 2. REPORT TYPE | 3. DATES COVERED |
|---|---|---|
| October G013 | Annual | 30Septemàer2012– G9Septemàer2013 |

**4. TITLE AND SUBTITLE**

Noninvasive Detection and Differentiation of Axonal Injury/Loss, Demyelination, and Inflammation

**5a. CONTRACT NUMBER**

**5b. GRANT NUMBER**
W81XWH-12-1-0457

**5c. PROGRAM ELEMENT NUMBER**

**6. AUTHOR(S)**

Sheng-Kwei Song, Joong Hee Kim, Peng Sun, Yong Wang, Anne Cross

**5d. PROJECT NUMBER**

**5e. TASK NUMBER**

**5f. WORK UNIT NUMBER**

E-Mail: ssong@wustl.edu

**7. PERFORMING ORGANIZATION NAME(S) AND ADDRESS(ES)**

Washington University
Campus Box 8018
660 South Euclid Ave.
St. Louis, MO 63110-1010

**8. PERFORMING ORGANIZATION REPORT NUMBER**

**9. SPONSORING / MONITORING AGENCY NAME(S) AND ADDRESS(ES)**
U.S. Army Medical Research and Materiel Command
Fort Detrick, Maryland 21702-5012

**10. SPONSOR/MONITOR'S ACRONYM(S)**

**11. SPONSOR/MONITOR'S REPORT NUMBER(S)**

**12. DISTRIBUTION / AVAILABILITY STATEMENT**
Approved for Public Release; Distribution Unlimited

**13. SUPPLEMENTARY NOTES**

**14. ABSTRACT**

In the current proposal, in vivo diffusion basis spectrum imaging (DBSI) was employed to simultaneously quantify CNS white matter pathologies of axonal injury, demyelination, and inflammation, correlating with postmortem immunohistochemical staining, in experimental autoimmune encephalomyelitis (EAE) and cuprizone treated mice. During the first year of this study, we struggled with the lengthy data acquisition (> 5 hours in previously published paper). Despite the previous success, it proved to be very difficult to maintain consistent data quality using the old protocol. We thus developed a revised protocol taking the advantage of simple structure of optic nerve and corpus callosum to reduce the diffusion weighting scheme to 25 directions, shortened the acquisition time by ~50%. Our preliminary data from the cuprizone treated mice suggested that reduction in acquisition time indeed had significant impact in data quality for imaging corpus callosum since the RF coil could not be improved at the present time. However, preliminary results also support that the new scheme is sufficient to reflect the known pathologies in corpus callosum under the influence of cuprizone treatment. We have observed through the in vivo DBSI results axon and myelin pathologies seen by histology and EM that wer not reported by other MRI approaches. With the improved RF coil and the reduced diffusion weighting scheme, we found that the new protocol worked perfectly for mouse optic nerve DBSI measurements as outline in the proposal.

We have identified various vendors of the FDA approved anti-inflammatory drug treating relapse-remitting MS, Gilenya (finfolimod, or FTY720), for animal studies. Thus, we would like to request the pre-approval to replace our initially proposed use of dexamethasone with Gilenya to increase the clinical relevance of the current proposal.

**15. SUBJECT TERMS**
Multiple sclerosis, diffusion basis spectrum imaging, diffusion tensor imaging, EAE, inflammation, axonal injury, curizone, demyelination

| 16. SECURITY CLASSIFICATION OF: | | | 17. LIMITATION OF ABSTRACT | 18. NUMBER OF PAGES | 19a. NAME OF RESPONSIBLE PERSON USAMRMC |
|---|---|---|---|---|---|
| **a. REPORT** | **b. ABSTRACT** | **c. THIS PAGE** | UU | 7 | **19b. TELEPHONE NUMBER** *(include area code)* |
| U | U | U | | | |

# Table of Contents

## Introduction

Accumulating literature evidence suggests that the MS disability associated with acute MS relapses is related to the combined effect of the underlying inflammation, axonal injury, and demyelination, while long-term MS disability is due to the extent of permanent axonal damage, independent of the frequency or severity of relapses([1-10]). In the current proposal, *in vivo* diffusion basis spectrum imaging (DBSI) was employed to simultaneously quantify CNS white matter pathologies of axonal injury, demyelination, and inflammation, correlating with postmortem immunohistochemical staining, in experimental autoimmune encephalomyelitis (EAE) and cuprizone treated mice.
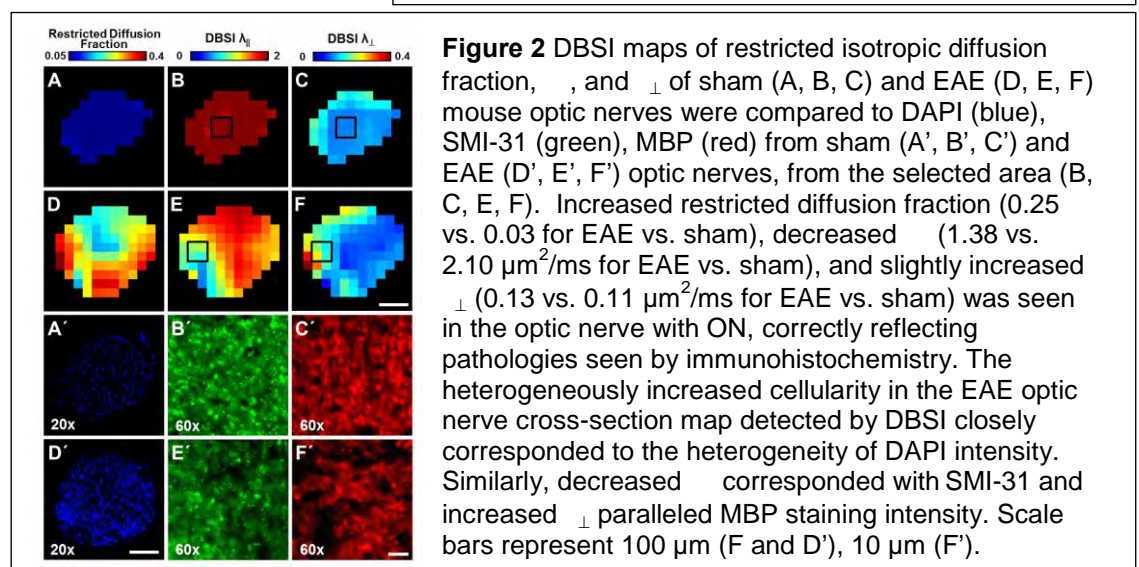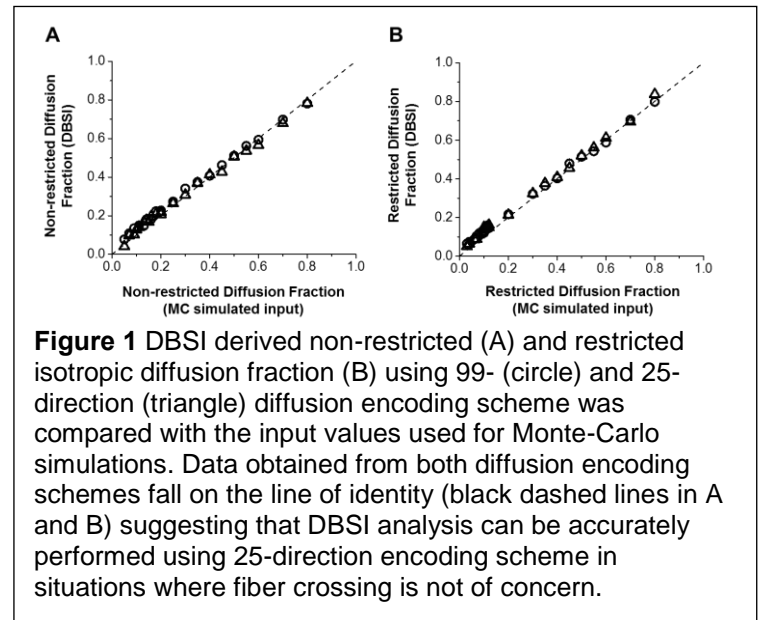
## Body

The approved statement of work for the year one covers all tasks proposed in specific aim 1 "Longitudinal DBSI evaluation of evolving pathology of corpus callosum from mice treated with cuprizone for 0, 4, and 8 weeks followed by 4, and 8 weeks of recovery. Cross sectional DBSI studies will be performed on the same longitudinal time points for histology validation of DBSI findings. (Months 1 – 14)". In the following we will describe steps we took in preparation for performing the proposed studies and results from our efforts.

*1. A simplified diffusion scheme was developed to shorten acquisition time.*

Despite our previous success in acquiring diffusion basis spectrum imaging (DBSI) data using the 99-direction diffusion weighting scheme (~5-hour acquisition) for cross-sectional *in vivo* studies (*11*), a team member raised the concern of the protocol for longitudinal studies. We thus performed preliminary tests and developed a simplified diffusion weighting scheme to shorten the acquisition time of the previously proposed protocol by ~50%.

To image the coherent white matter tracts without fiber crossing, such as optic nerve and corpus callosum, a reduced scanning time can be achieved by significantly reducing the number of diffusion weighted images. Thus, we adopted a 25-direction diffusion encoding scheme (*12*) to assess the effect of extra-fiber structural and pathological components confounding diffusion tensor imaging (DTI) computation using data generated by both Monte-Carlo simulations and DBSI measurements on fixed tissue phantoms. Increased extent of vasogenic edema was mimicked by addition of various amount of gel to fixed normal trigeminal nerves or by increasing non-restricted isotropic diffusion tensor component in Monte-Carlo simulations. Increased cellularity was simulated by graded increase of restricted isotropic diffusion tensor component in Monte-



**Figure 1** DBSI derived non-restricted (A) and restricted isotropic diffusion fraction (B) using 99- (circle) and 25-direction (triangle) diffusion encoding scheme was compared with the input values used for Monte-Carlo simulations. Data obtained from both diffusion encoding schemes fall on the line of identity (black dashed lines in A and B) suggesting that DBSI analysis can be accurately performed using 25-direction encoding scheme in situations where fiber crossing is not of concern.
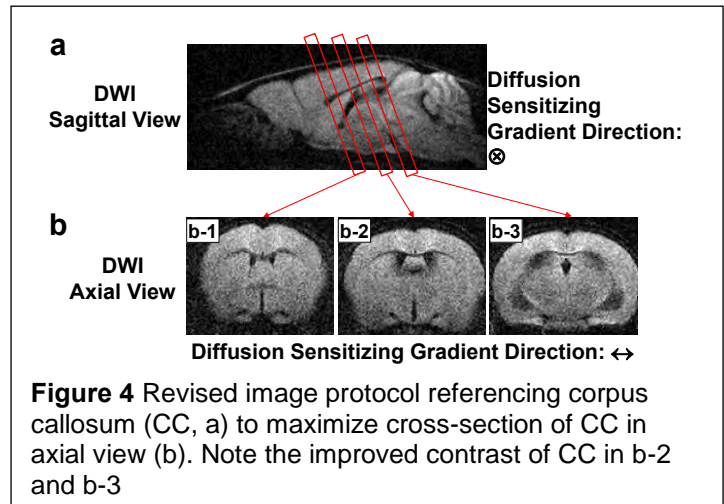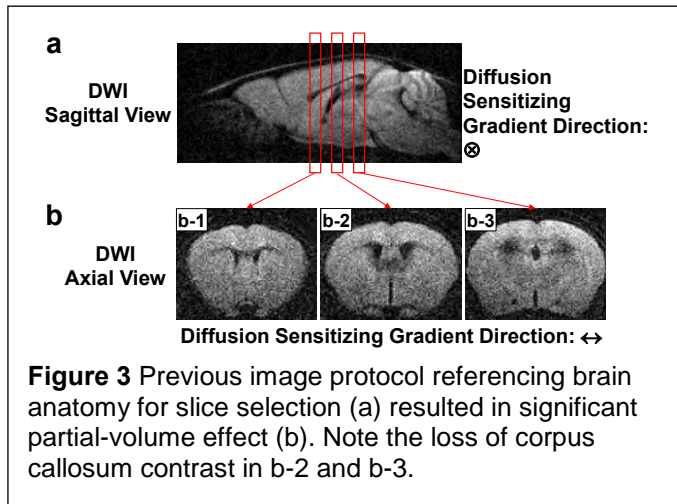
Carlo simulations. Results suggested that the 25-direction diffusion scheme provided accurate DBSI estimation of both fiber diffusion parameters and extra-fiber cellularity/edema extent (Fig. 1). An *in vivo* 25-direction DBSI analysis was performed on EAE optic nerve as an example to demonstrate the



**Figure 2** DBSI maps of restricted isotropic diffusion fraction, ∥, and ⊥ of sham (A, B, C) and EAE (D, E, F) mouse optic nerves were compared to DAPI (blue), SMI-31 (green), MBP (red) from sham (A', B', C') and EAE (D', E', F') optic nerves, from the selected area (B, C, E, F). Increased restricted diffusion fraction (0.25 vs. 0.03 for EAE vs. sham), decreased ∥ (1.38 vs. 2.10 µm$^2$/ms for EAE vs. sham), and slightly increased ⊥ (0.13 vs. 0.11 µm$^2$/ms for EAE vs. sham) was seen in the optic nerve with ON, correctly reflecting pathologies seen by immunohistochemistry. The heterogeneously increased cellularity in the EAE optic nerve cross-section map detected by DBSI closely corresponded to the heterogeneity of DAPI intensity. Similarly, decreased ∥ corresponded with SMI-31 and increased ⊥ paralleled MBP staining intensity. Scale bars represent 100 µm (F and D'), 10 µm (F').

validity of derived DBSI parameters with post-imaging immunohistochemistry verification (Fig. 2). Thus, 25-direction diffusion weighting scheme was selected for the proposed studies.

2. *Improved image planning was optimized to reduce partial-volume effect.*
In the previously published report on cross-sectional *in vivo* DBSI of cuprizone treated mice, significant partial volume was noted (Fig. 3). To reduce the potential complication from the partial-volume effect in the studies outline in statement-of-work for aim 1, imaging protocol tests were performed to optimize image planning (Fig. 4).



**Figure 3** Previous image protocol referencing brain anatomy for slice selection (a) resulted in significant partial-volume effect (b). Note the loss of corpus callosum contrast in b-2 and b-3.



**Figure 4** Revised image protocol referencing corpus callosum (CC, a) to maximize cross-section of CC in axial view (b). Note the improved contrast of CC in b-2 and b-3

3. *Longitudinal and Cross-sectional DBSI of corpus callosum (CC) at 0, 6, 12 weeks of cuprizone feeding followed by 6 and 12 weeks of recovery.*
During a visit to the Uniformed Services University of the Health Sciences meeting with Dr. Regina Armstrong (Director of Center for Neuroscience and Regenerative Medicine, and Professor of Anatomy, Physiology and Genetics) who is a renowned expert in curpizone mouse model and a long-time collaborator, the PI was advised to modify the initially proposed time course to match the "norm" in the field. After a further discussion with team members, we decided to perform our studies matching the time course most commonly used by others in the field. The revised time course lengthens the study by 2 months but our results will match previous and future studies in the field (Table 1). In addition, a parallel cross-sectional DBSI-IHC study was also performed to match DBSI results with IHC validation (Table 2).

| Table 1. Summary of Longitudinal DBSI | | | | | |
|---|---|---|---|---|---|
| weeks | 0 (baseline) | 6 | 12 | 12 + 6 | 12 + 12 |
| Control (number of mice) | 6 | No scans scanner down | 6 | 4 (2 mice died before imaging) | 4 (to complete at $1^{st}$ week of Nov.) |
| Cuprizone (number of mice) | 8 | No scans scanner down | 7 (1 mouse died before week 12) | 7 | 7(to complete at $1^{st}$ & $2^{nd}$ week of Nov.) |

| Table 2. Summary of Cross-Sectional DBSI-IHC | | | | |
|---|---|---|---|---|
| | | 6 weeks | 12 weeks | 12 + 6 weeks |
| Completed | Control | 3 | 3 | 2 |
| | Cuprizone | 3 | 3 | 3 |
| Ongoing | Control | 3 ($3^{rd}$ week Nov, 2013) | 3 ($3^{rd}$ week Dec, 2013) | 3 ($2^{nd}$ week Feb, 2014) |
| | Cuprizone | 3 ($3^{rd}$ week Nov, 2013) | 3 ($3^{rd}$ week Dec, 2013) | 3 ($2^{nd}$ week Feb, 2014) |

Preliminary results suggested that in the absence of significant cell infiltration as seen in the previous report of 4-week cuprizone treatment DTI derived axial and radial diffusivity performed reasonably well as seen by DBSI at 6, 12, and 12+6 weeks. Consistent with our previous findings, axonal injury detected by DTI largely recovered based on DTI derived axial and radial diffusivity. Although the absolute value of axial and radial diffusivity was different from those derived by DBSI, the general trend reflecting axonal and myelin integrity has been comparable between DTI and DBSI (Fig. 5). However, DBSI derived isotropic diffusion tensor components clearly revealed tissue structural changes that were not visible by DTI (Fig. 6). Specifically, the

extent of increased cellularity in cuprizone treated animals at 6, 12, and 12+6 weeks was significantly decreased comparing with those seen at 4-week as previously reported (*11, 13*). Most interestingly, both longitudinal and cross-sectional animals showed clear increase in non-restricted isotropic diffusion tensor component (putatively corresponding to vasogenic edema, tissue loss, or increased inter-axonal space resulting from reduced axonal caliber). Currently, all cross-sectional study animals have been perfusion fixed and sectioned. All IHC staining was performed and images captured ready for quantification. The longitudinal end point, 12 + 12 weeks, animals will also serve as the cross-section end point histology. The quantification will start after the 12 + 12 weeks animals are sectioned and stained.
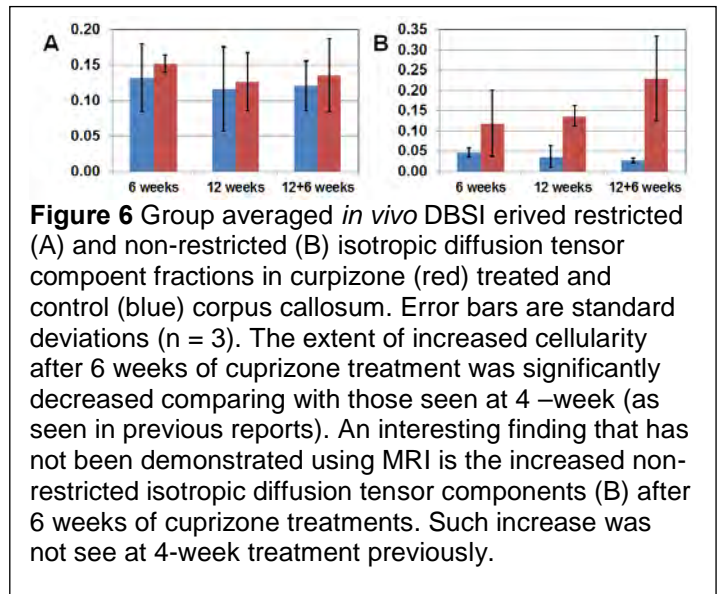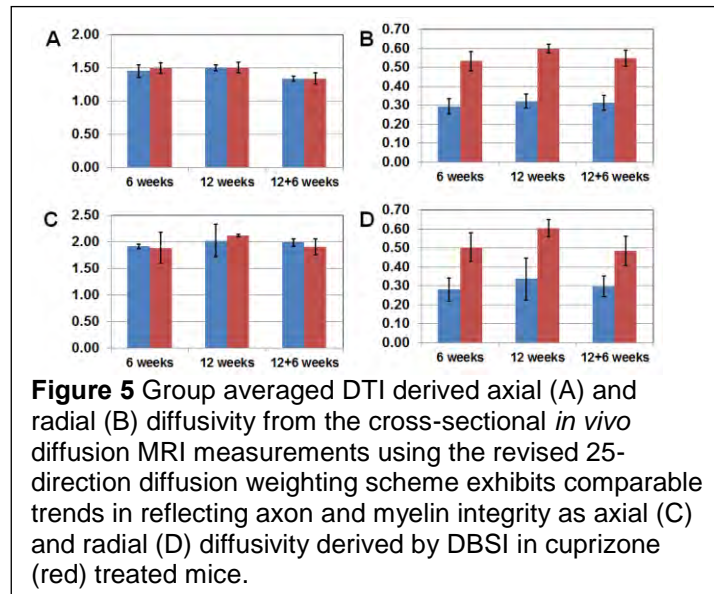


**Figure 5** Group averaged DTI derived axial (A) and radial (B) diffusivity from the cross-sectional *in vivo* diffusion MRI measurements using the revised 25-direction diffusion weighting scheme exhibits comparable trends in reflecting axon and myelin integrity as axial (C) and radial (D) diffusivity derived by DBSI in cuprizone (red) treated mice.



**Figure 6** Group averaged *in vivo* DBSI erived restricted (A) and non-restricted (B) isotropic diffusion tensor compoent fractions in curpizone (red) treated and control (blue) corpus callosum. Error bars are standard deviations (n = 3). The extent of increased cellularity after 6 weeks of cuprizone treatment was significantly decreased comparing with those seen at 4 –week (as seen in previous reports). An interesting finding that has not been demonstrated using MRI is the increased non-restricted isotropic diffusion tensor components (B) after 6 weeks of cuprizone treatments. Such increase was not see at 4-week treatment previously.

**Key Research Accomplishments**
- Established a simplified diffusion weighting scheme to perform DBSI analysis on coherent white matter tracts such as optic nerve and corpus callosum (targets of this work), and spinal cord.
- Improved DBSI computation algorithm to shorten the time required for analysis by more than 10 folds.
- Changes in inter-axonal environment, may reflect previously seen axonal structural changes in EM (*13*), were detected by *in vivo* DBSI that was not seen previously by DTI or other MRI techniques.
- Established experimental protocol for *in vivo* DBSI of mouse optic nerves as described in statement-of-work of years 2 and 3.

**Reportable Outcomes**
Currently, we do not have any reportable outcomes in terms of scientific publications. The longitudinal DBSI studies on cuprizone treated mice turned out to be more challenging than cross-sectional measurement or expected. After initial setbacks, we are now close to the end of the time course study. Hopefully, we may have one or two reportable outcomes in the format of publications in next report.

**Conclusion**
In the first year of this funding support, we have overcome the challenge of lengthy *in vivo* diffusion MRI measurements of mouse corpus callosum by developing an abbreviated data acquisition protocol. This was achieved by performing phantom studies as well as Monte-Carlo simulations assuming all targeted tissues, i.e., optic nerve and corpus callosum, in this proposal are coherent without fiber crossing. Our results suggested that the 25-direction diffusion weighting scheme was perfect for mouse optic nerve measurements outlined in this proposal. However, for mouse corpus callosum measurements the signal-to-noise ratio may be at the low end where DBSI analysis may not be as accurate as those obtained by the 5-hour data acquisition. Our preliminary results suggested that current protocol although not perfect is sufficient to detect structural changes (known by classical histology and EM) that were not reported by other MRI methods. Thus, we are confident that in completion of the proposed study we will be able to establish DBSI as the future diffusion MRI method for noninvasive detection of CNS pathologies and structural changes.

In anticipating the future work of this proposal, we would like to request the approval of using the FDA approved anti-inflammatory drug, Gilenya® (fingolimod, or FTY720), instead of the proposed use of dexamethasone to increase the clinical relevance of the current proposal.

# References

1. O. Andersen, Predicting a window of therapeutic opportunity in multiple sclerosis. *Brain* **133**, 1863 (Jul, 2010).
2. C. Bjartmar, G. Kidd, S. Mork, R. Rudick, B. D. Trapp, Neurological disability correlates with spinal cord axonal loss and reduced N-acetyl aspartate in chronic multiple sclerosis patients. *Ann Neurol* **48**, 893 (Dec, 2000).
3. C. Confavreux, S. Vukusic, Natural history of multiple sclerosis: a unifying concept. *Brain* **129**, 606 (Mar, 2006).
4. C. S. Constantinescu, B. Gran, Multiple sclerosis: autoimmune associations in multiple sclerosis. *Nat Rev Neurol* **6**, 591 (Nov, 2010).
5. D. S. Conway, J. A. Cohen, Multiple sclerosis: Mechanisms of disability accumulation in multiple sclerosis. *Nat Rev Neurol* **6**, 654 (Dec, 2010).
6. L. K. Fisniku *et al.*, Disability and T2 MRI lesions: a 20-year follow-up of patients with relapse onset of multiple sclerosis. *Brain* **131**, 808 (Mar, 2008).
7. J. M. Frischer *et al.*, The relation between inflammation and neurodegeneration in multiple sclerosis brains. *Brain* **132**, 1175 (May, 2009).
8. A. Kutzelnigg *et al.*, Cortical demyelination and diffuse white matter injury in multiple sclerosis. *Brain* **128**, 2705 (Nov, 2005).
9. A. Scalfari *et al.*, The natural history of multiple sclerosis: a geographically based study 10: relapses and long-term disability. *Brain* **133**, 1914 (Jul, 2010).
10. B. D. Trapp, K.-A. Nave, Multiple Sclerosis: An Immune or Neurodegenerative Disorder? *Annual Review of Neuroscience* **31**, 247 (2008).
11. Y. Wang *et al.*, Quantification of increased cellularity during inflammatory demyelination. *Brain* **134**, 3587 (2011).
12. P. G. Batchelor, D. Atkinson, D. L. Hill, F. Calamante, A. Connelly, Anisotropic noise propagation in diffusion tensor MRI sampling schemes. *Magn Reson Med* **49**, 1143 (Jun, 2003).
13. M. Xie *et al.*, Rostrocaudal analysis of corpus callosum demyelination and axon damage across disease stages refines diffusion tensor imaging correlations with pathological features. *J Neuropathol Exp Neurol* **69**, 704 (Jul, 2010).